2014 IEEE International Conference on Robotics & Automation (ICRA)
Hong Kong Convention and Exhibition Center
May 31 - June 7, 2014. Hong Kong, China

Bracing the Human Body with Supernumerary Robotic Limbs for Physical Assistance and Load Reduction

Federico Parietti, Kameron Chan and H. Harry Asada, *Member, IEEE*

***Abstract*— A new approach to physically assisting the human with a wearable robot is presented. Supernumerary Robotic Limbs (SRLs) attached to the human waist support the body efficiently when the human is taking fatiguing postures, e.g. hunching over, squatting, or reaching the ceiling. Unlike a leg exoskeleton, where powered joints are attached to the human joints and are constrained to move together with the human limb, the SRL can take an arbitrary posture to maximize the load bearing efficiency. Taking a near-singular configuration, the SRL can bear a large load with small power consumption. First, the "bracing" strategy for supporting the human body is described, followed by a mathematical analysis of the load bearing efficiency. The optimal SRL posture and joint torques are then obtained in order to minimize the human load. Numerical and experimental results using a prototype of the SRL demonstrate the effectiveness of the method.**

I. INTRODUCTION

Industrial automation has revolutionized a wide range of production processes, from car manufacturing to microprocessor fabrication. However, one of the most technologically advanced industry sectors – aircraft manufacturing – has so far made a limited use of robotic technology, and relies heavily on skilled workforce. In this paper we present the design and control strategy of a wearable robot aimed to assist aircraft assembly workers, augmenting their capabilities and reducing their workload.

Human workers are essential for aircraft assembly because of three main reasons. First, the assembly process is characterized by a wide range of complex tasks and by a flexible schedule, which must be modified if the need for reworks arises. Trained workers have the capability to easily learn new tasks, and the flexibility to coordinate with each other and modify their work plans. Second, aircraft assembly entails the use of special scaffolds and tools designed for human workers. Traditional industrial robots do not meet the size and safety requirements to operate in such tight spaces, cannot operate hand tools, and are not capable of quickly navigating through complex scaffolds. Third, the large size of aircraft and their small lot size (compared to mass consumer goods) excludes the use of traditional automated assembly lines where the process is decomposed into simple independent operations that can be execute by industrial robots.

Fig. 1. Concept of the Supernumerary Robotic Limbs (SRL), a wearable robot that extends its user's body with two additional robotic arms.

Although the aircraft assembly process requires abilities that are unique to human workers – such as learning and flexibility – it would also benefit from advantages of robotic technology like precision and strength. In particular, many assembly tasks impose a heavy workload on humans, resulting in fatigue and injury and decreased productivity [1]. For example, lifting large parts and operating heavy tools require exerting significant forces for prolonged periods of time. Moreover, working on hard-to-reach locations such as the floor or the ceiling of the aircraft fuselage forces humans to assume uncomfortable postures – stooped, crouched, or stretched. These requirements become even more problematic if we consider that aircraft assembly workforce is characterized by a particularly marked aging trend, with a median age of about 48 years [2].

In this context, it would be beneficial to provide workers with robotic assistants able to help with the most physically demanding tasks, while leaving humans in complete control of the assembly process. If these robotics assistants were wearable, they could reach an unprecedented level of coordination with the human users, eventually becoming functional extensions of their bodies. To realize this vision, we designed and built the Supernumerary Robotic Limbs (SRL), a wearable robot which augments its wearer by providing two additional robotic arms [3] [4]. Unlike traditional

This work was supported in part by The Boeing Company

F. Parietti is with the Department of Mechanical Engineering, Massachusetts Institute of Technology, Cambridge, MA 02139, USA parietti at mit.edu

K. Chan is with the Department of Mechanical Engineering, Massachusetts Institute of Technology, Cambridge, MA 02139, USA kcchan at mit.edu

H. Asada is with Faculty of Mechanical Engineering, Massachusetts Institute of Technology, Cambridge, MA 02139, USA asada at mit.edu

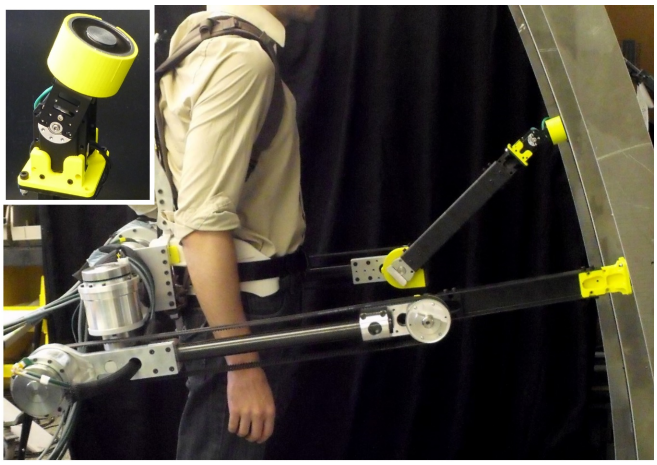

Fig. 2. The SRL prototype. A 3D printed waist brace connects the robot to the lower back of the user. Three series viscoelastic actuators and a servo control the robotic arm degrees of freedom (two in the shoulder, one in the elbow, one in the wrist). The elbow actuator trasmits torque to its joint through two timing belts. The insert shows the model of the servo-actuated wrist, equipped with an electromagnetic gripper.

upper or lower limb exoskeletons, where powered joints are attached to the corresponding human joints, the SRL is not constrained to follow the movements of the human (Figure 1). Its robotic limbs are free to move independently, and can therefore assume the posture that best helps the wearer. This unique characteristic of the SRL has been exploited in order to stabilize the user during tasks that require high accuracy [5]. In this paper we present a method for supporting the human upper body when the worker has to stoop or crouch for a long time. By bracing the body against a wall, floor, and other structures the SRL can effectively bear the upper body load during fatiguing tasks. Furthermore, we show that the independent kinematic structure of the SRL allows for more efficient load bearing compared to leg exoskeletons.

The paper is organized as follows. Section II briefly describes the design concept of the SRL. Section III introduces a bracing strategy for load bearing, and analyzes the power efficiency and load bearing capacity of SRLs in comparison with leg exoskeletons. Section IV formulates an optimization problem for finding an optimal posture and torque distribution of SRL so that the human effort for bearing the load may be a minimum. Section V discusses and extends the optimization results. Finally, Section VI summarizes the most important contributions of this study.

II. ROBOT DESIGN

The SRL consists of a pair of wearable robotic limbs that can intuitively and safely assist the human (Figure 2). A detachable 3D printed waist brace forms the interface between the human and the SRLs base structure. Its ergonomic shape ensures that the robot rests on the iliac crest, the thick edge of the hip bone, and that the robots weight is directed to the legs and away from the spine [4]. Shoulder straps and a waist belt secure the SRL to the user. Each robotic limb is attached to a side of the base structure, and is provided with 4 degrees of freedom – two near the base (shoulder), one in the middle (elbow), and one at the end effector (wrist). The range of the robot joints allows the end effectors to reach the majority of the human limbs workspace (both legs and arms) in order to provide assistance where needed.

The specifications of the joints are designed to match human performance in terms of torque and weight [3]. The shoulder flexion joint, which is the most powerful joint and has to lift objects in front of the human, has a 270-degree range of motion and a maximum torque of 69 Nm. The shoulder abduction and elbow flexion joints, which are orthogonal to the shoulder flexion joint and experience little gravity load, have a maximum torque of 39 Nm. The shoulder abduction joint has a 90-degree range of motion, while the elbow flexion joint has a 180-degree range of motion. Each joint is actuated by a brushless DC motor through a Harmonic Drive gearbox (50:1).

To minimize the robotic limbs moment of inertia and to reduce power consumption, the elbow actuator is placed immediately behind the shoulder as a counterweight. Torque is then transmitted to the elbow using two 12 mm wide, 5 mm pitch GT2 timing belts. The robotic arms are designed to allow internal routing of signal and power wires for the end effectors. A series viscoelastic element having stiffness of 153 Nm/rad is placed between each joint and its gearbox. This added elasticity a) decouples the gearbox and motor, b) provides low-cost and robust torque sensing (using encoders to measure deflection), and c) guarantees safety in case of impact [6] [7] [8]. The viscoelastic element, made of polyurethane rubber, allows the achievement of the desired joint stiffness with a significant reduction in mass and size with respect to a traditional steel coil spring [3].

One additional degree of freedom is placed at the wrist, and controlled with a servo motor. The robotic arm can be equipped with various end effectors, tailored for different tasks. For this study, an electromagnet (weight: 275 g, max holding force: 490.5 N) is mounted on the wrist output flange (see Figure 2, insert). The electromagnet allows the robotic arm to easily make contact with the environment. The wrist actuator is used to orient the outer surface of the magnet (a disk with D = 50 mm) so that it is parallel to the desired surface of contact. The magnetic force is then activated and guarantees a firm grip. This hoding system is faster and avoids the extra weight and complexity of a robotic gripper or hand. If the environment does not present any ferromagnetic surfaces, a vacuum gripper (such as the Joulin FlexiGrip GS120) could replace the electromagnetic end effector. Vacuum can be created with a Venturi valve, using the compressed air system available in the aircraft factory.

III. BRACING AND LOAD BEARING ANALYSIS

A. The Bracing Strategy

Workers in the aircraft assembly process must perform complex tasks, requiring high precision and substantial physical effort. The SRL assists the human in these demanding

situations, increasing their accuracy and reducing their fatigue. In this section we present the strategy used by the SRL to provide support to the wearer, and analyze the effectiveness of load bearing in comparison to exoskeletons.

Unlike an exoskeleton, where powered joints are attached to the human joints and move together with the human, the Supernumerary Robotic Limbs can make contact with the environment at any point within their workspace. By grasping or clamping structural elements such as aircraft beams or safety scaffolds, they can secure the human body to the environment, and thereby suppress disturbances and lower the load to be borne by the human. In other words, this strategy allows the robot to brace the human body against an external structure. Therefore, we call it the "bracing strategy".

In a previous study, the bracing strategy has been applied to increase the equivalent stiffness at the hip of the user, thereby reducing disturbances and increasing accuracy [5]. In this paper, we will apply the bracing strategy in order to minimize the torques that the human joints must exert to hold a weight or to keep an uncomfortable position. An exemplary case study considered in this paper is to support an aircraft assembly worker in performing a task on the floor or at a very low position of the airplane structure. Examples of such tasks include fuselage assembly, routing wires, fastening seats, and performing quality checks. All of these operations require holding a crouched position for extended periods of time, suppressing oscillatory movements, and stabilizing the body in order to guarantee the precision of the task execution. Maintaining uncomfortable postures may accelerate fatigue of the workers, reducing their productivity and even posing risks to their health [1]. Wearable robots such as exoskeletons or the SRL can be used to support the workers and reduce their fatigue. In this study, we will focus on load bearing capacity and compare the efficiency and effectiveness of SRLs bracing strategy against leg exoskeletons. We consider the case where the worker is standing in front of the aircraft fuselage with both feet in contact with the floor, and the torso is leaning forward in order to perform the assembly task at a low position.

Figure 3 shows the kinematic model used for analyzing the load bearing characteristics of the SRL bracing strategy compared to a leg exoskeleton. Four simplifying assumptions have been adopted in the analysis of the problem. First, the model is composed by rigid links and rotational joints, and neglects the compliance of the human-robot interface. It also lumps SRL base and human torso in a single rigid body. These simplifications are possible because small deflections due to compliance do not influence the static distribution of torques between the robot and the human, which is the objective of this analysis. Second, we assume that the robot can securely grip the environment, e.g. a fuselage structure, so that no slip occurs at the contact point. This can be achieved using an electromagnet whose holding force can generate enough static friction to secure the grip (see Section II). Third, the analysis assumes that the robot links as well as the human and exoskeleton links are mass less. The effect of link mass can be included, but it makes the analysis unnecessarily complex. Finally, the model considers half of the human-robot system: it includes one human leg and one robotic limb.

As shown in Figure 3, the system consists of one SRL, human leg and torso. The position and orientation of the human torso that is aligned with the SRL base is denoted by a 3-dim vector, $p = [x_G, y_G, \beta_{torso}]^T$. The human torso combined with the SRL base link weights m kg with a center of mass above the SRL base. This creates a gravity load, $f_{x,ext} = 0\,,\ f_{y,ext} = -mg$, as well as a moment about the hip joint, $\tau_{ext} = mgd_w \cos(\beta_{torso})$. Collectively, the external load to be borne by the human and the robot is expresses by a 3-dim vector, $F_{ext} = [f_{x,ext}, f_{y,ext}, \tau_{ext}]^T$.

B. Load Bearing Analysis

The basic equations that describe the static torque-force relationships of the system are as follows. For the robotic limb, the endpoint forces F_R are related to the joint torques τ_R by the Jacobian matrix

$$\tau_R = J_R^T F_R \tag{1}$$

where the vector τ_R contains the torques at the joints of the robotic arm (wrist, elbow and shoulder). An analogous expression can be written for the human leg. In this case, the torques are referred to the ankle, knee and hip joints of the human. The expressions of the robot and human Jacobians J_R and J_H are reported in Appendix A.

Consider the total power consumed at the SRL for bearing the load. The power consumption can be written as

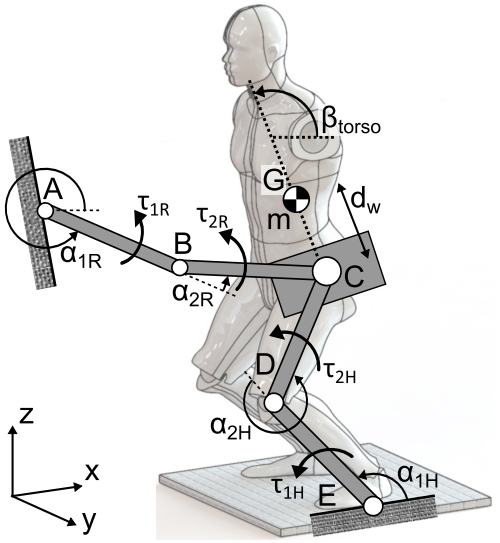

Fig. 3. The model used to study the bracing strategy. All the angles are measured at the joints, except for β_{torso} which indicates the orientation of the human torso with respect to the x axis. Points A and B represent the SRL wrist and elbow. Points D and E represent the human knee and ankle. Point C represents both the SRL shoulder and the human hip. τ_{3R} and τ_{3H}, the torques exerted at the hip respectively by the SRL arm and the human leg, are not drawn here. Point G is the center of mass of the human torso. The general model is 3D. Its 2D projection on the xz plane is used in the computational example (Figures 4 and 5).

$$P_R = \tau_R^T W_R \tau_R \tag{2}$$

where W_R is a weighting matrix, which is positive-definite and symmetric. In case DC motors with torque constant K_{ti}, armature resistance R_{ti}, and gear ratio $1 : r_i$ ($r_i > 1$) are used for individual joints $i = 1, \dots, n_R$, the weighting matrix is given by

$$W_R = diag\left(\frac{R_1}{r_1^2 K_{t1}^2}, \dots, \frac{R_n}{r_n^2 K_{tn}^2}\right) \tag{3}$$

Substituting (1) into (2) yields

$$P_R = F^T J_R W_R J_R^T F \tag{4}$$

For comparison we consider an exoskeleton attached along the human leg, exerting joint torques on the human leg joints. The power consumption at the exoskeleton can be derived in a similar manner,

$$P_E = F^T J_E W_E J_E^T F \tag{5}$$

Notice that $J_E = J_H$, because the exoskeleton is constrained to follow the human leg kinematics. Our special interest is to assist the human when he/she has to squat in order to reach a very low point, as illustrated in Figure 3. At this posture, the exoskeleton, which has to take the same posture as the human, is not advantageous; the exoskeleton must bear the load in the same way as the human. To compare the load bearing efficiency, consider the quotient between the two: P_R/P_E,

$$\eta = \frac{P_R}{P_E} = \frac{F^T J_R W_R J_R^T F}{F^T J_E W_E J_E^T F} = \frac{F^T A F}{F^T B F} \tag{6}$$

where A and B are real, symmetric matrices given by

$$A \triangleq J_R W_R J_R^T \ , \ B \triangleq J_E W_E J_E^T \tag{7}$$

It is expected that the quotient η is smaller than 1 if the SRL takes a proper posture by bracing the human body against a wall, the floor, or a structure that it can contact. It is natural to assume that the posture of the exoskeleton as well as the human leg is not singular when half way crouching, as illustrated in Figure 3. Therefore, matrix B is assumed non-singular. Since the matrix A is symmetry and the matrix B is symmetry and non-singular, the quotient can be treated as a Rayleigh Quotient. Finding the minimum of the quotient is a generalized eigenvalue problem, and is given by the smallest eigenvalue of the following matrix:

$$\eta_{min} = \lambda_{min}(B^{-1}A) \tag{8}$$

If the SRL is at a singular configuration, it can bear a load with zero power consumption, as long as the load vector F is in the null space of matrix A:

$$\eta_{min} = 0 \ , \ P_R = 0 \ \text{ for } \ F \in N(A) \tag{9}$$

The Rayleigh quotient is small even at a non-singular SRL configuration, if the SRL posture is near singular and the load vector is nearly aligned with the null space of matrix A.

The SRL can take various configurations. Finding a right posture for bracing the human body is critically important for lowering the Rayleigh quotient, i.e. efficient load bearing. The following section will address how to find the right posture that optimizes the metric subject to constraints on available surfaces to brace.

IV. OPTIMIZATION

A. Introduction

In order to maintain a static posture, aircraft assembly workers must compensate for their own weight and for the forces originated operating tools or moving parts. These actions generate an equivalent force and torque vector $-F_{ext}$ at the hip, which must be borne by the legs of the worker generating an equal and opposite vector F_{ext}.

When the SRL is used, F_{ext} can be provided in part or entirely by the robot, relieving the human:

$$F_{ext} = F_H + F_R \tag{10}$$

where F_R and F_H are the hip forces and torques generated respectively by the robot and the human. The joint torques required to originate these hip forces can be calculated using the Jacobian matrices of the robot and of the human leg (J_R and J_H), considered as two link manipulators fixed to the ground at their contact points.

The total force to be generated at the hip can thus be written as

$$F_{ext} = \begin{bmatrix} J_R^{-T} & J_H^{-T} \end{bmatrix} \begin{bmatrix} \tau_R \\ \tau_H \end{bmatrix} = M \, \tau_{tot} \tag{11}$$

Both τ_R and τ_H are vectors with three elements, corresponding to the torques of the robot and human joints. Since the rank of M is at most 3, its null space has at least dimension 3. This means that there are infinite couples of τ_R and τ_H that originate the same F_{ext}. In other words, the human leg and the SRL arm form with the ground a closed kinematic chain that has infinite static solutions for the joint torques.

The objective of the SRL arm is to minimize the human workload. Among the infinite possible τ_R given a particular system configuration, we thus want to determine the value that minimizes τ_H. The vector of the human joint torques can be written as

$$\tau_H = J_H^T(F_{ext} - J_R^{-T}\tau_R) \tag{12}$$

, where $J_H^T F_{ext}$ represents the torques that the human leg should provide to generate F_{ext} without any external help, and the second term represents the torques that the action of the SRL subtracts from the human workload.

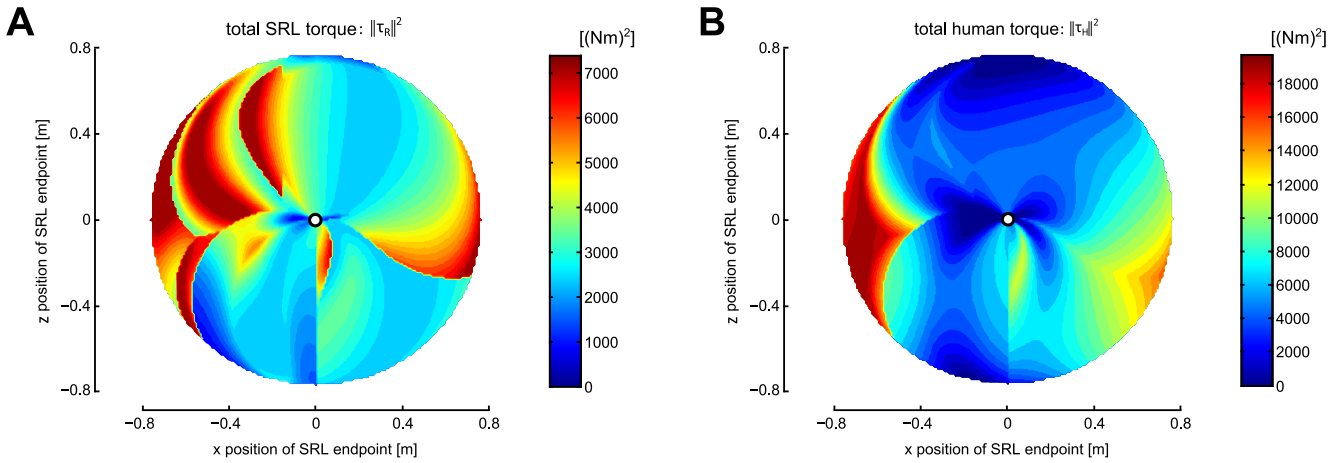

Fig. 4. A) Squared norm of the optimal SRL torques $\|\tau_R\|^2$ and B) corresponding human workload $\|\tau_H\|^2$, plotted for every possible contact point of the SRL end with the environment. The central white dot represents the SRL shoulder (point C in Figure 3). The best bracing configurations for the SRL are the ones that lead to $\|\tau_H\|^2 = 0$ - the blue areas in B) - and also required limited robot torques - the blue areas in A). It is possible to observe that both conditions are respected when making contact the environment at either the bottom or the top of the SRL workspace (see Section V).

B. Problem Statement

Find an optimal posture and joint torques of the SRL that minimize the power required for the human to bear the external load, F_{ext} , subject to torque limits of the SRL and the admissible joint angles, $\theta_R \in D_R$:

$$\theta_R^{opt} = \arg \min_{\substack{\theta \in D_R \\ |\tau_R| \leq \tau_{R,max}}} P(F_R; \theta_R) \tag{13}$$

where

$$P(F_R; \theta_R) = \|\tau_H\|^2 = (F_{ext} - F_R)^T J_H W_H J_H^T (F_{ext} - F_R) \tag{14}$$

C. Optimization

The analytical expression of τ_R which minimizes $\|\tau_H\|^2 = \tau_H^T \tau_H$ can be done by finding the point where the derivative of $\|\tau_H\|^2$ is zero. The complete derivation is detailed in Appendix B.

However, this solution does not take into account the limits to the torques of the robotic arm. There might be situations in which the joint torques required to originate F_{ext} and minimize the human workload ($\|\tau_H\|^2 = 0$) exceed the maximum torques that can be provided by the SRL actuators. Moreover, the limits of the different actuators are different (See Appendix C for the characteristics of the SRL actuators and the model parameters). In particular, the robot wrist joint is the weakest both because its actuator is the smallest and because its gripper must guarantee the no-slip condition at the base of the bracing model. In order to include these limits in the solution, we solve constrained optimization problems employing the method of the Lagrange Multipliers.

The analysis so far has been general, and holds for the general 3D problem. We will now present the analytical solution to the optimization process in the 2D case. We consider the projection of the man-machine system on the sagittal plane (plane xz, see Figure 3). Although the movements of the human and the robot are three dimensional, a planar model can adequately represent both the kinematic configuration necessary to reach a crouched position and the major joint torques required to bear gravitational loads.

The iterative procedure to find τ_R which minimizes $\|\tau_H\|^2$ and respects the SRL torque limits is as follows. The human and robot configuration (J_H and J_R) are given. We start computing the solution τ_R^* which makes $\|\tau_H\|^2$ zero (the global minimum). This solution is acceptable provided that it respects all the torque limits. If this is not true, three cases may happen.

First, one element of τ_R^* exceeds its maximum value torque $\tau_{iR,max}$. In this case we apply the Lagrange Multipliers to minimize $\|\tau_H\|^2$ with the the constraint that $\tau_{iR} <= \tau_{iR,max}$, resulting in the Lagrangian:

$$L = \|\tau_H\|^2 - \lambda(\tau_{iR}^2 - \tau_{iR,max}^2) \tag{15}$$

This optimization yields a new value of τ_R^*, with τ_{iR} saturated to its maximum value (for the analytical expression of the solution, see Appendix D).

Second, if two elements of τ_R^* exceed their maximum values $\tau_{iR,max}$ and $\tau_{jR,max}$, we apply the Lagrange Multipliers to minimize $\|\tau_H\|^2$ with two corresponding constraints, resulting in the Lagrangian:

$$L = \|\tau_H\|^2 - \lambda(\tau_{iR}^2 - \tau_{iR,max}^2) - \mu(\tau_{jR}^2 - \tau_{jR,max}^2) \tag{16}$$

This optimization yields a new value of τ_R^*, with τ_{iR} and τ_{jR} saturated to their maximum values (for the analytical expression of the solution, see Appendix D).

Third, if all three elements of τ_R^* exceed their maximum values, then we find the solution that minimizes $\|\tau_H\|^2$ among the eight triples $[\pm\tau_{1R,max}\,, \pm\tau_{2R,max}\,, \pm\tau_{3R,max}]^T$. This procedure is repeated until all the elements of τ_R^* are within their

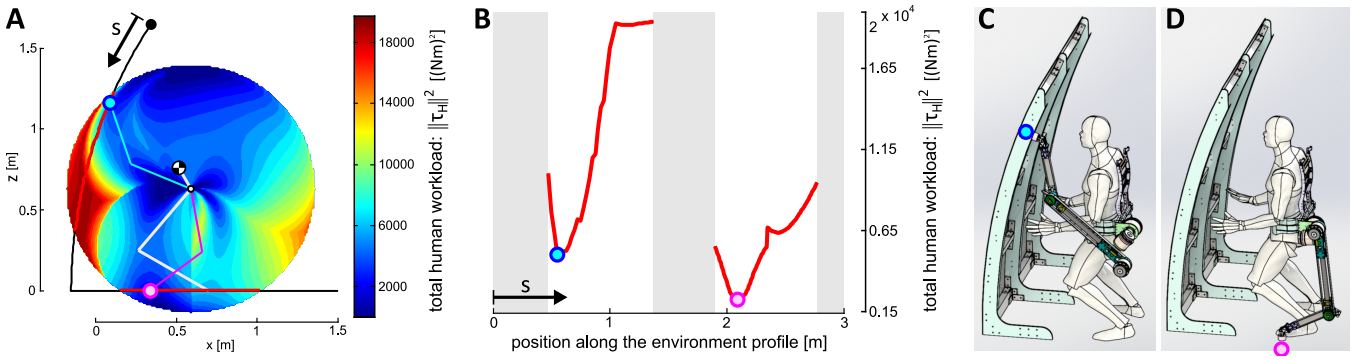

Fig. 5. Finding the optimal SRL configuration with limited contact points. A) The human workload $\|\tau_H\|^2$ map is overlapped with the profile of an aircraft structure (black line). The human configuration is drawn with grey lines, while the optimal SRL bracing configurations are drawn with magenta and cyan lines. The red curves represent the available contact points – the intersection between the environment profile and the robot workspace. B) The value of $\|\tau_H\|^2$ in the available contact points is plotted against coordinate s (the position of the contact points along the ground profile). The grey areas represent the segments of the environment that cannot be reached by the SRL. The magenta dot is the contact point that minimizes $\|\tau_H\|^2$. The cyan dot is a local minimum of $\|\tau_H\|^2$, which can be used if it is preferable to grasp the wall instead of the floor. C) SRL bracing configuration corresponding to the local minimum on the wall (cyan point). D) SRL bracing configuration corresponding to the global minimum among the available contact points (magenta point, on the floor). Notice that the available contact points do not include the most advantageous ones (placed at the bottom and at the top of the SRL workspace, see Section V).

limits. Figure 4 shows the squared norm $\|\tau_R^*\|^2$ of the solutions obtained for every possible configuration in the workspace of the SRL. The position of the human is fixed ($\alpha_{1H} = 150°$, $\alpha_{2H} = -100°$, $\beta_{torso} = 120°$). The figure also shows the corresponding values of $\|\tau_H\|^2$.

In practice, though, it is not necessary to find τ_R^* and the corresponding $\|\tau_H\|^2$ for every point in the workspace of the robot. It suffices to intersect the SRL workspace and the available contact points with the environment. One such situation is shown in Figure 5, where the environment profile represents the floor and the wall inside an aircraft hull. For every contact point that can be reached by the robot, we compute τ_R^* and $\|\tau_H\|^2$ with the method detailed above. The optimal contact point (and robot configuration) is the one that minimizes the human workload $\|\tau_H\|^2$. If many solutions realize the same minimum workload, the one requiring minimum robot torques $\|\tau_R^*\|^2$ is selected among them. It is important to remark that this optimization method can be applied with any kind of environment profile. It is not necessary to have the contact point that yields the global minimum of $\|\tau_H\|^2$ (blue area in Figure 4B). If limited contact points are available, the algorithm selects within that subset the point that locally minimizes $\|\tau_H\|^2$.

V. DISCUSSION

A. Comparison

In order to compare the performance of the SRL in reducing the human workload with that of a traditional exoskeleton, three scenarios will be analyzed. First, we consider the case of a worker without any robotic aid. We calculate the torques that the human joints must exert in order to compensate for the weight of the user.

Second, we consider the case of a worker wearing a traditional exoskeleton. In this scenario, the man-machine system must generate joint torques that compensate for the weight of both the human and the robot. The exoskeleton torques will be subtracted from the required total ankle, knee and hip torques. The goal is to minimize the absolute value of the residual torques, which must be originated by the human joints. In order to have a fair comparison, the weight and maximum torques of the exoskeleton are chosen to be the same as the ones of the SRL.

Third, we consider the case in which the worker is wearing the SRL, which employs the bracing strategy in order to minimize the workload of the user. We select for the robotic arm the optimal configuration that has been found in the previous section (configuration colored in magenta in Figure 5). In all of the three cases the position of the human is the same (joint angles equal to those considered in Section IV). This uniquely defines also the position of the exoskeleton, whose kinematics are the same as those of the wearers leg. The SRL, conversely, is free to select the optimal bracing configuration. The results in terms of human workload are reported in Table I.

The computed human torques indicate that, although wearing an exoskeleton is more advantageous than not using any robotic aid, the SRL provides the best performance in terms of human workload minimization. The intuitive explanation of the advantage of the SRL in bearing the load is that, by choosing a configuration close to the singular one, the robotic arm can support the wearer without resorting to large joint torques. The load is simply discharged to the ground through the robotic structure. In the vicinity of the singularity the

TABLE I
HUMAN WORKLOAD COMPARISON

joint torque	only human	human and exoskeleton	human and SRL
τ_{1H} $[Nm]$	-59	-43	-10
τ_{2H} $[Nm]$	79	57	34
τ_{3H} $[Nm]$	-24	0	-29
$\|\tau_H\|^2$ $[(Nm)^2]$	10298	5098	2097

SRL exploits a large mechanical advantage in order to bear loads with the least effort.

The power consumption of the SRL prototype arm while bearing a vertical load has been measured in several configurations. The considered robot positions and the results in terms of required power are shown in Figure 6. These experimental results confirm that bearing a load in the vicinity of a singular configuration requires the least amount of joint torques and therefore of power.

B. Bracing With Two Robotic Arms

Until this point, we have applied the bracing strategy to a single SRL arm. If the user is executing a task, in fact, the help of the other SRL arm might be needed in order to get aircraft parts or to handle heavy tools. When the task does not require specific robotic help, however, both SRL arms can be used to brace the user and minimize the human body workload. In this case the SRL can always compensate the full body weight with optimal efficiency. By assuming a triangular configuration (Figure 7), the SRL can keep both robotic arms in a singular configuration and compensate all the gravitational forces with minimal joint torques (the residual moment arms at the wrist and at the shoulder are very small by design). The only limiting factor is the strength of the end effector electromagnets, whose size can be tailored to the load to be borne. This triangular bracing strategy is efficient for any COM height h (Figure 7), therefore confirming the advantage of the SRL over traditional exoskeletons.

VI. CONCLUSIONS

This paper presented a novel strategy for the use of the Supernumerary Robotic Limbs (SRL), a wearable robot designed to assist human wearers by augmenting their bodies with two additional robotic arms. Our vision for the SRL is to become a functional extension of the wearers body, coordinating with the user to execute complex operations and providing support during the most physically demanding tasks. In this study, we focus on the use of the SRL to minimize the torques required to the human joints while maintaining an uncomfortable posture or bearing a static load.

We developed the bracing strategy, which consist of the SRL making contact with the environment in order to support the user. By grasping the environment, the robot is able to reduce the static loads borne by the wearer. As a consequence, the torques required to the human joints can be minimized. We presented a method to identify the optimal SRL bracing configuration, which allows to minimize human effort while taking in account the robot torque limits and the available contact points with the environment.

Finally, we showed that the SRL can minimize user workload with a limited power consumption. This can be achieved because the kinematic independence of the SRL allows it to choose the optimal available bracing point. A traditional exoskeleton, on the other hand, is constrained to follow the movements of the human leg and thus cannot select an optimal configuration, resulting in higher robot joint torques and risk of saturation. We conclude that the SRL has the potential to provide optimal support to the human user in an efficient way.

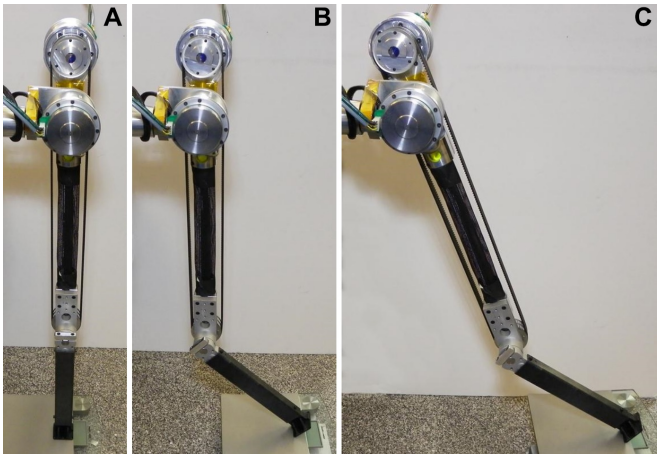

Fig. 6. The experimental setup used to measure the power consumption of the SRL arm while bearing vertical loads. We compare three different configurations in terms of power required to bear one Newton of vertical load. In case A) the required power was 0.04 $[W/N]$, in case B) it was 0.53 $[W/N]$ and in case C) it was 0.77 $[W/N]$.

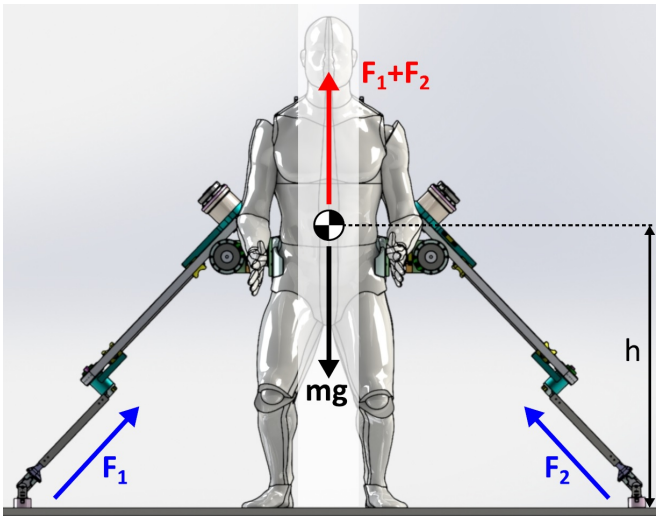

Fig. 7. Bracing with two robotic arms. The triangular bracing strategy guarantees efficient gravitational load compensation for every h.

APPENDIX A

The expression of the SRL arm Jacobian is

$$J_R = \begin{bmatrix} -l_{1R}\,s_{1R} - l_{2R}\,s_{12R} & -l_{2R}\,s_{12R} & 0 \\ l_{1R}\,c_{1R} + l_{2R}\,c_{12R} & l_{2R}\,c_{12R} & 0 \\ 1 & 1 & 1 \end{bmatrix}$$

, where

$$\begin{cases} s_{1R} = \sin(\alpha_{1R}) \\ c_{1R} = \cos(\alpha_{1R}) \end{cases} \text{ and } \begin{cases} s_{12R} = \sin(\alpha_{1R} + \alpha_{2R}) \\ c_{12R} = \cos(\alpha_{1R} + \alpha_{2R}) \end{cases}$$

The expression of the human leg Jacobian J_H is analogous, but it employs the leg joint angles (α_{1H}, α_{2H} and α_{3H}) and the leg link lengths (l_{1H} and l_{2H}).

APPENDIX B

We want to minimize $\|\tau_H\|^2 = \tau_H^T \tau_H$. Its complete expression is

$$\|\tau_H\|^2 = [J_H^T F_{ext} - J_H^T J_R^{-T} \tau_R]^T [J_H^T F_{ext} - J_H^T J_R^{-T} \tau_R]$$

, which can be expanded into

$$\|\tau_H\|^2 = F_{ext}^T J_H J_H^T F_{ext} - 2 F_{ext}^T J_H J_H^T J_R^{-T} \tau_R + \\ + \tau_R^T J_R^{-1} J_H J_H^T J_R^{-T} \tau_R$$

The derivative $\frac{\mathrm{d}\|\tau_H\|^2}{\mathrm{d}\tau_R}$ can be calculated applying the following properties

$$\begin{cases} \frac{\partial c^T \tau_R}{\partial \tau_R} = c \\ \frac{\partial \tau_R^T C \tau_R}{\partial \tau_R} = 2\, C\, \tau_R \end{cases}$$

Where c is a vector and C is a symmetric square matrix:

$$\begin{cases} c = J_R^{-1} J_H J_H^T F_{ext} \\ C = J_R^{-1} J_H J_H^T J_R^{-T} \end{cases}$$

Therefore the derivative can be written as

$$\frac{\mathrm{d}\,\|\tau_H\|^2}{\mathrm{d}\tau_R} = 2\, C\, \tau_R - 2\, c$$

Equating this expression to zero and premultiplying by $(J_H J_H^T)^{-1} J_R$ yields the critical point

$$\tau_R = J_R^T F_{ext}$$

APPENDIX C

Limits of the SRL actuators:

SRL joint i	1 (wrist)	2 (elbow)	3 (shoulder)
max torque $\tau_{iR,max}$ $[Nm]$	30	40	70

The dimensions of the SRL links are $l_{1R} = l_{2R} = 0.4\,m$. The dimensions of the human kinematic chain are $l_{1H} = l_{2H} = 0.5\,m$, and $d_w = 0.15\,m$. The total mass m (human and SRL base) is $40\,kg$. The mass of the human is $32.5\,kg$. Note that we consider half of the human-machine system (see Section 3).

APPENDIX D

A. One Constraint

If $|\tau_{1R}^*| > \tau_{1R,max}$, we use the Lagrangian

$$L = \|\tau_H\|^2 - \lambda(\tau_{1R}^2 - \tau_{1R,max}^2)$$

This leads to the following two solutions for the constrained minimization of $\|\tau_H\|^2$

$$\tau_{1R,solutions} = [\tau_{1\mathrm{Rmax}},\ -\tau_{1\mathrm{Rmax}}]^T$$

$$\tau_{2R,solutions} = \begin{bmatrix} -\frac{C_{23}\,c_3 - C_{33}\,c_2 + C_{21}\,C_{33}\,\tau_{1\mathrm{Rmax}} - C_{23}\,C_{31}\,\tau_{1\mathrm{Rmax}}}{C_{22}\,C_{33} - C_{23}\,C_{32}} \\ -\frac{C_{23}\,c_3 - C_{33}\,c_2 - C_{21}\,C_{33}\,\tau_{1\mathrm{Rmax}} + C_{23}\,C_{31}\,\tau_{1\mathrm{Rmax}}}{C_{22}\,C_{33} - C_{23}\,C_{32}} \end{bmatrix}$$

$$\tau_{3R,solutions} = \begin{bmatrix} \frac{C_{22}\,c_3 - C_{32}\,c_2 + C_{21}\,C_{32}\,\tau_{1\mathrm{Rmax}} - C_{22}\,C_{31}\,\tau_{1\mathrm{Rmax}}}{C_{22}\,C_{33} - C_{23}\,C_{32}} \\ \frac{C_{22}\,c_3 - C_{32}\,c_2 - C_{21}\,C_{32}\,\tau_{1\mathrm{Rmax}} + C_{22}\,C_{31}\,\tau_{1\mathrm{Rmax}}}{C_{22}\,C_{33} - C_{23}\,C_{32}} \end{bmatrix}$$

, where c_i and C_{ij} are respectively the elements of vector c and the elements of matrix C (see Appendix B). An analogous constrained optimization method can be applied if τ_{2R} or τ_{3R} exceed their limits.

B. Two Constraints

If $|\tau_{1R}^*| > \tau_{1R,max}$ and $|\tau_{2R}^*| > \tau_{2R,max}$:

$$L = \|\tau_H\|^2 - \lambda(\tau_{1R}^2 - \tau_{1R,max}^2) - \mu(\tau_{2R}^2 - \tau_{2R,max}^2)$$

This leads to the following two solutions for the constrained minimization of $\|\tau_H\|^2$

$$\tau_{1R,solutions} = [\tau_{1\mathrm{Rmax}},\ \tau_{1\mathrm{Rmax}},\ -\tau_{1\mathrm{Rmax}},\ -\tau_{1\mathrm{Rmax}}]^T$$

$$\tau_{2R,solutions} = [\tau_{2\mathrm{Rmax}},\ -\tau_{2\mathrm{Rmax}},\ \tau_{2\mathrm{Rmax}},\ -\tau_{2\mathrm{Rmax}}]^T$$

$$\tau_{3R,solutions} = \begin{bmatrix} -\frac{C_{31}\,\tau_{1\mathrm{Rmax}} - c_3 + C_{32}\,\tau_{2\mathrm{Rmax}}}{C_{33}} \\ \frac{c_3 - C_{31}\,\tau_{1\mathrm{Rmax}} + C_{32}\,\tau_{2\mathrm{Rmax}}}{C_{33}} \\ \frac{c_3 + C_{31}\,\tau_{1\mathrm{Rmax}} - C_{32}\,\tau_{2\mathrm{Rmax}}}{C_{33}} \\ \frac{c_3 + C_{31}\,\tau_{1\mathrm{Rmax}} + C_{32}\,\tau_{2\mathrm{Rmax}}}{C_{33}} \end{bmatrix}$$

An analogous constrained optimization method can be applied if τ_{1R} and τ_{3R} or τ_{2R} and τ_{3R} exceed their limits.

REFERENCES

[1] T. M. Brown, "Injuries, illnesses and fatalities in manufacturing, 2005," Bureau of Labor Statistics, July 2007.

[2] A. Mosisa and S. Hipple, "Trends in labor force participation in the united states," *Monthly Labor Review*, vol. 129(10), pp. 35–57, 2006.

[3] B. Llorens-Bonilla, F. Parietti, and H. Asada, "Demonstration-based control of supernumerary robotic limbs," in *Proc. IEEE Int. Conference on Intelligent Robots and Systems*, 2012.

[4] C. Davenport, F. Parietti, and H. Asada, "Design and biomechanical analysis of supernumerary robotic limbs," in *ASME Dynamic Systems and Control Conference*, 2012.

[5] F. Parietti and H. Asada, "Dynamic analysis and state estimation for wearable robotic limbs subject to human-induced disturbances," in *Proc. IEEE Int. Conference on Robotics and Automation*, 2013, in press.

[6] J. F. Veneman, R. Ekkelenkamp, R. Kruidhof, F. C. Van Der Helm, and H. Van Der Kooij, "A series elastic- and bowden-cable-based actuation system for use as torque actuator in exoskeleton-type robots," *Int. J. Rob. Res.*, vol. 25, no. 3, pp. 261–281, Mar. 2006.

[7] F. Parietti, G. Baud-Bovy, E. Gatti, R. Riener, L. Guzzella, and H. Vallery, "Series viscoelastic actuators can match human force perception," *Mechatronics, IEEE/ASME Transactions on*, vol. 16, no. 5, pp. 853 –860, oct. 2011.

[8] A. Bicchi, M. Bavaro, G. Boccadamo, D. De Carli, R. Filippini, G. Grioli, M. Piccigallo, A. Rosi, R. Schiavi, S. Sen, and G. Tonietti, "Physical human-robot interaction: Dependability, safety, and performance," in *Advanced Motion Control, 2008. AMC '08. 10th IEEE International Workshop on*, march 2008, pp. 9 –14.